Electronic Supplementary Information

Facet Ratio Engineering of CuO Dictates C_{2+} Products Selectivity in CO_2 Electroreduction

Xu Yang,[†a] Wei Fan,[†a] Jiayao Fan,[a,b] Chongyang Zhou,[a] Lizhi Jiang,[a] Naien Shi,[a,c,*] and Min Han[a,b,*]

[a]Strait Institute of Flexible Electronics (SIFE, Future Technologies), Fujian Key Laboratory of Flexible Electronics, Fujian Normal University, Fuzhou 350117, China

[b]Jiangsu Key Laboratory of Biofunctional Materials, School of Chemistry and Materials Science, Nanjing Normal University, Nanjing 210023, China

[c]State Key Laboratory of Organic Electronics and Information Displays & Institute of Advanced Materials (IAM), Nanjing University of Posts& Telecommunications, 9 Wenyuan Road, Nanjing 210023, China

[†]X. Yang, and W. Fan contributed equally.

*To whom correspondence should be addressed.

E-mail: ifeneshi@fjnu.edu.cn (Prof. N. Shi); ifemhan@fjnu.edu.cn (Prof. M. Han)

Experimental section

Chemicals. The copper (II) nitrate trihydrate ($Cu(NO_3)_2 \cdot 3H_2O$, > 99%), Urea (> 99%), potassium hydroxide (> 85%), 1-Butanol (G. R. grade), Isopropanol (G. R. grade), and Ethanol (G. R. grade) were purchased from Sinopharm Chem. Reagent Co. Ltd. And the sodium dodecyl sulfate (SDS, > 99%) and Nafion D-520 dispersion (5 wt%) were bought from ThermoFisher (China) Scientific Co. Ltd. All chemicals were used as received that without further purification. All aqueous solutions were prepared with deionized water (18.25 MΩ·cm).

Synthesis of CuO-1. In a typical synthesis, the $Cu(NO_3)_2 \cdot 3H_2O$ (5 mmol) and SDS (280 mg) were dissolved in a mixed solution of 25 mL H_2O and 25 mL 1-Butanol, and stirred continuously for 30

minutes. Then, 3 g urea was added to above solution and stirred continuously for 30 minutes, too. The stirred solution was transferred to a round-bottomed flask and heated it in an oil bath to 110 ^{o}C and reacted for 24 h. After separated by centrifugation and washed three times with deionized water and ethanol, the CuO-1 was collected, and finally dried under vacuum (400 mg in theory, 387.3 mg in fact, yield: 96.8%).

Synthesis of CuO-2. For each synthesis, 150 mg of pre-synthesized CuO-1 in oil bath at 110^{o}C were added into a clean ceramic boat, which is placed into the central region of a horizontal tube furnace. Subsequently, the furnace was heated to 300 ^{o}C under air with the heating rate of 3 °C min^{-1}, and maintained that temperature for 3 h. After naturally cooled down to room temperature, the sample was collected, and used for characterizations and tests (150 mg in theory, 146.6 mg in fact, yield: 97.7%).

Synthesis of CuO-3. In a typical procedure, the $Cu_2(OH)_2CO_3$ precursors were firstly prepared via hydrothermal method. Specifically, the $Cu(NO_3)_2 \cdot 3H_2O$ (5 mmol) and SDS (280 mg) were dissolved in a mixed solution of 25 mL H_2O and 25 mL 1-Butanol, and stirred continuously for 30 min. Then, 3 g urea was added to the above solution and continuously stirred for 30 min. Afterward, the mixed solution was transferred to a 100 mL stainless-steel autoclave and reacted at 80 ℃ for 24 h. After naturally cooled down to room temperature, the products were separated by centrifugation, washed with deionized water and ethanol for three times, and finally dried under vacuum, and the $Cu_2(OH)_2CO_3$ precursors were obtained (555 mg in theory, 502.4 mg in fact, yield: 90.5%). Then 150 mg of $Cu_2(OH)_2CO_3$ were subjected to annealing at 300^{o}C in air for 3h to obtain CuO-3 (108.1 mg in theory, 104.7 mg in fact, yield: 96.9%). The detailed annealing treatment procedure was the same as that for CuO-2.

Materials characterization. The catalysts were characterized by powder X-ray diffraction (PXRD), X-ray photoelectron spectroscopy (XPS), Raman spectrum, X-ray absorption structure (XAS), scanning electron microscopy (SEM), transmission electron microscopy (TEM), high-resolution TEM (HRTEM), Energy-dispersive X-ray Spectra (EDS). Powder X-ray diffraction (PXRD) patterns were recorded on a Miniflex-600 diffractometer using Cu Kα radiation (λ = 0.154 nm). XPS analysis

was performed on the Thermo Scientific ESCA Lab 250Xi using 200 W monochromatic Al Kα radiation. The 500 μm X-ray spot was used. The base pressure in the analysis chamber was about 3×10^{-10} mbar. Typically, the hydrocarbon C1s line at 284.8 eV from adventitious carbon was used for energy referencing. Raman measurements were carried out using a HORIBA JY LabRAM HR Evolution Raman microscope (λ = 532 nm). The XAS spectra (Cu K-edge) were collected at BL11B station in Shanghai Synchrotron Radiation Facility (SSRF), China. Using fixed-exit Si (111) double-crystal monochromator, the data collection was carried out in fluorescence mode using ionization chamber. The morphologies of the samples were observed on a JEOL ARM200F (JEOL, Japan) operated at an acceleration voltage of 200 kV with a cold-filled emission gun and double hexapole Cs correctors (CEOS GmbH, Germany). And SEM was carried out on HITACHI SU8000 at an accelerating voltage of 5 kV.

Electrode preparation. 20 mg of obtained catalysts, 1 mL of isopropanol and 50 μL of Nafion ionomer solution (5 wt%) were first mixed and sonicated for 1 h to obtain the uniform catalyst inks. Then, the catalyst inks were sprayed onto the glassy carbon electrode and dried in N_2 flow. Thus, the catalysts modified working electrodes were fabricated. The catalyst loading on the electrode was fixed to be 1 mg·cm^{-2}.

Electrochemical measurements. Electrochemical experiments were implemented in a designed flow cell with two compartments separated by anion-exchange membrane (FAB-PK-130) and employed 1 M KOH as electrolyte. In the flow cell, a peristaltic pump was used to control the flow rate of the electrolyte at 20 mL·min^{-1}. The CO_2 flow rate was controlled at 30 sccm by a mass flow controller. The cathode electrolyte chamber was equipped with a cathode consisting of a carbon paper coated catalyst (1×1 cm^2) with a gas diffusion layer, along with Ag/AgCl reference electrodes. The linear sweep voltammetry (LSV) was tested at 5.0 mV·s^{-1} in the potential range of 0 to -1.0 V vs RHE. The CV curves were recorded in Ar-saturated 0.1 M $KHCO_3$ under the non-Faradaic potential region from 0.22 to 0.3 V vs Ag/AgCl with different scan rates (20, 60, 100, 140 and 180 mV·s^{-1}) to determine electrochemically active surface areas by calculating the double-layer capacitance (C_{dl}). The ratio of C_{dl} against the polycrystalline copper (29 μF·cm^{-2}) was calculated as the roughness

factor. [1, 2] All potentials reported in this paper were with respect to reversible hydrogen electrode (RHE), which were converted by the following equation: $E_{RHE} = E_{Ag/AgCl} + 0.198\ V + 0.059 \times pH$.

As for Pb-UPD measurements, all catalysts were subjected to pre-reduction treatment *via* two independent electrochemical protocols in an H-cell: cyclic voltammetry (CV) activation (40 cycles in the potential range of 0 to -1.2 V *vs*. RHE at a scan rate of 100 $mV \cdot s^{-1}$), and constant-potential reduction (held at -1.0 V *vs*. RHE for 1 h in CO_2-saturated 0.1 M $KHCO_3$ electrolyte).[3, 4] For Pb-UPD tests, the mixed electrolyte containing 0.1 M $NaClO_4$,10 mM $HClO_4$, and 3 mM $Pb(ClO_4)_2$ was prepared and employed for testing. Prior to characterization, the electrolyte was continuously purged with high-purity Ar. All the Pb-UPD experiments were carried out in H-cell with an Ag/AgCl electrode serving as the reference electrode. The related CV profiles were recorded at the potential window of -0.2 V to -0.6 V *vs*. Ag/AgCl with the scan rate of 10 $mV \cdot s^{-1}$. Additionally, the integrated Pb stripping charges of the three catalysts were calculated within the potential range of -0.47 V to -0.3 V *vs*. Ag/AgCl, with a copper foil served as the reference sample. The corresponding CV curves and the calculated Pb stripping charges were shown in **Fig. S24.**

***In-situ* Raman experiments.** The electrochemical Raman spectroscopy measurements were performed on a DXR2xi Raman microscope (Thermo Fisher), with a fixed excitation wavelength of 532 nm for all tests. All *in-situ* electrochemical Raman characterizations were implemented in a commercial electrolytic cell equipped with a quartz optical window (Gaoss Union Photoelectric Technology Co., Ltd.). The digital photographs for the configuration of *in-situ* Raman cell and the employed Raman spectrometer system were given in **Fig. S26**. Before the experiments, all the catalysts were uniformly coated on a glassy carbon electrode as the working electrode with the mass loading of 1 $mg \cdot cm^{-2}$. The Pt wire and an Ag/AgCl electrode were employed as the counter electrode and reference electrode, respectively. And the CO_2-saturated 0.1 M $KHCO_3$ aqueous solution was selected as the electrolyte. The in-situ Raman spectra for all catalysts were collected at a series of potentials, including the open-circuit potential (OCP), and -0.6 V to -1.0 V *vs* RHE. For all the experiments, the instrumental parameters were set as follows: the laser power of 15.0 mW, exposure time of 0.04 s (25 Hz), and an accumulation scan number of 120.

Product analyses. The gaseous products of electrochemical experiments were collected using a gas

sampling bag and analyzed by gas chromatography (GC, FuLi Technologies, GC9790). The GC with argon as the carrier gas was equipped with a thermal conductivity detector (for H_2) and a flame ionization detector (for CO, CH_4, C_2H_4, and C_2H_6). Quantification of the products was applied by external standard method. The liquid products were analyzed by ion chromatography (IC, ShengHan Technologies, Qingdao, CIC-100) and gas chromatography (GC, FuLi Technologies, GC9790). $HCOO^-$ and CH_3COO^- in the liquid products were detected by IC, while CH_3OH and C_2H_5OH were detected by GC. The quantification of the liquid products was applied by external standard method.

The Faradaic efficiency (FE) for gaseous products at each applied potential was calculated based on the following equations:

$$FE = (v_i \times P_0 \times V_0 \times z \times F)/(R \times T \times Q)$$

The Faradaic efficiency (FE) for liquid products at each applied potential was calculated based on the following equations:

$$FE = (C \times V_L \times z \times F)/Q$$

v_i: the fraction of gaseous products detected by GC;

P_0: the ambient pressure;

V_0: the analyzed gas volume in GC;

z: the number of transferred electrons for each product;

F: Faradaic constant, 96485 C mol^{-1}.

C: the molar concentration of liquid products in the sampling solution;

V_L: the catholyte volume;

Q: the total charge during the reaction.

Figures and captions

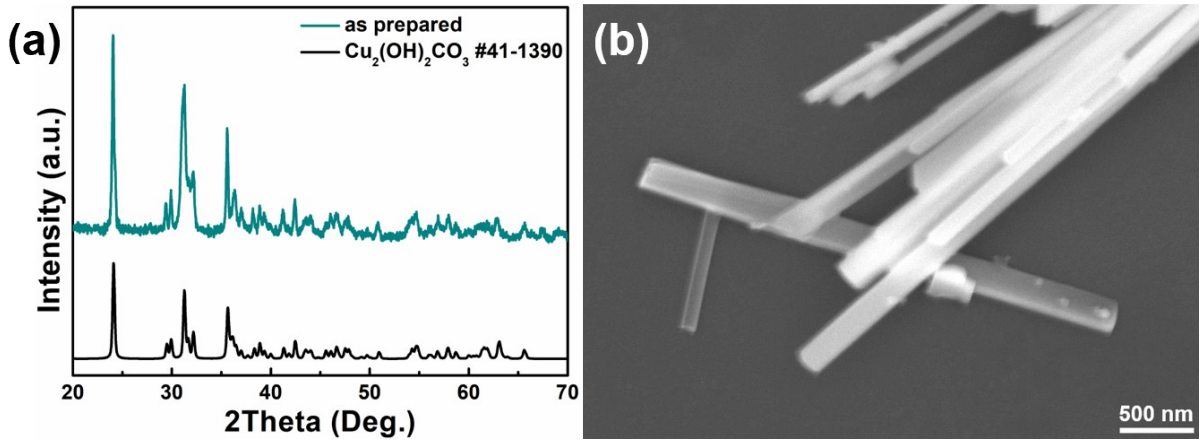

Fig. S1. The XRD pattern (a) and SEM image (b) for $Cu_2(OH)_2CO_3$ precursors.

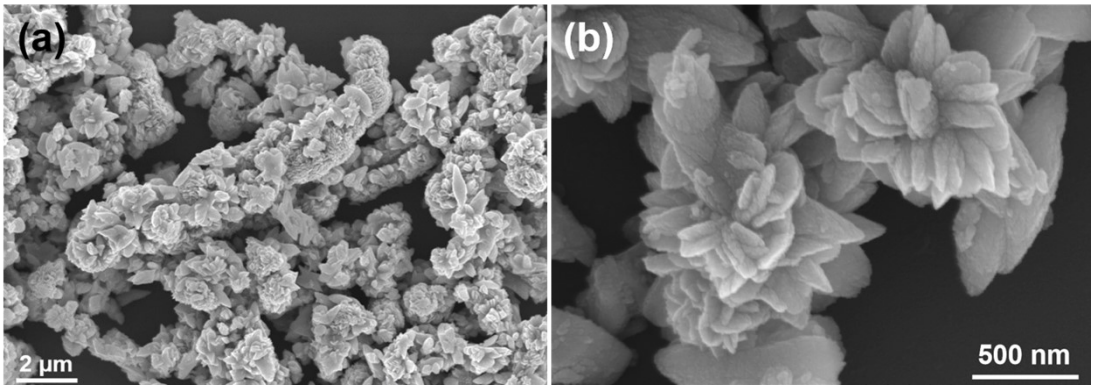

Fig. S2. The representative low-(a) and high-(b) magnification SEM images of CuO-1.

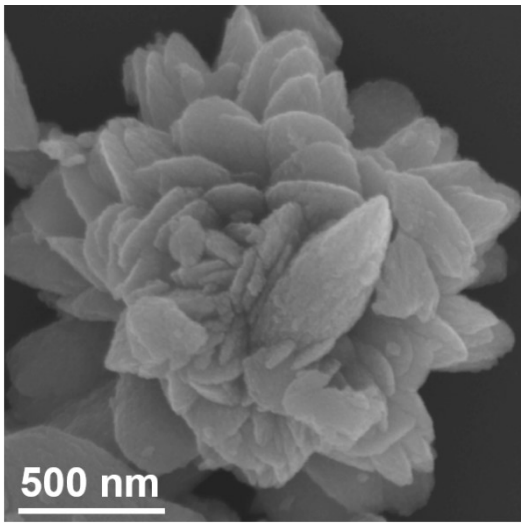

Fig. S3. The representative SEM image of CuO-2.

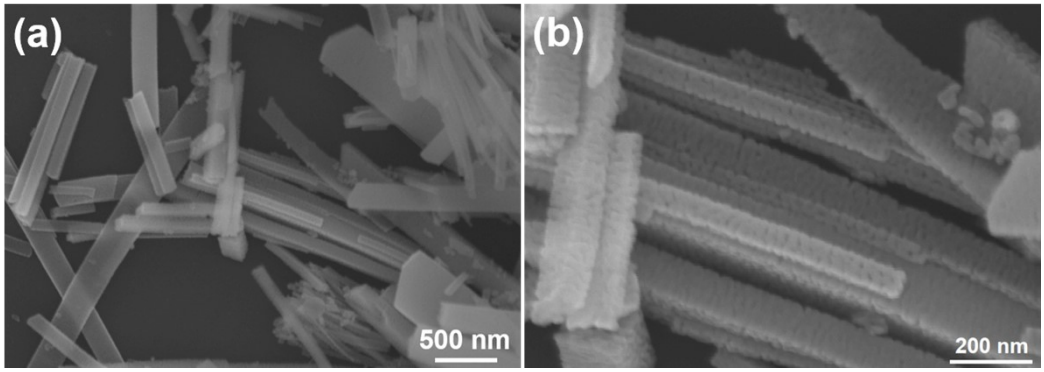

Fig. S4. The representative low-(a) and high-(b) magnification SEM images for CuO-3.

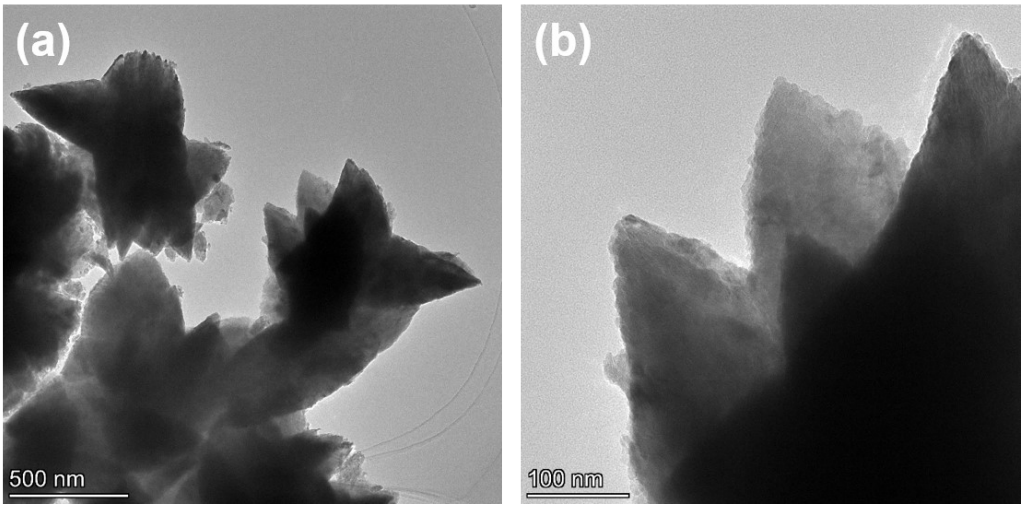

Fig. S5. (a,b) Low-(a) and high- (b) magnification TEM images of CuO-1.

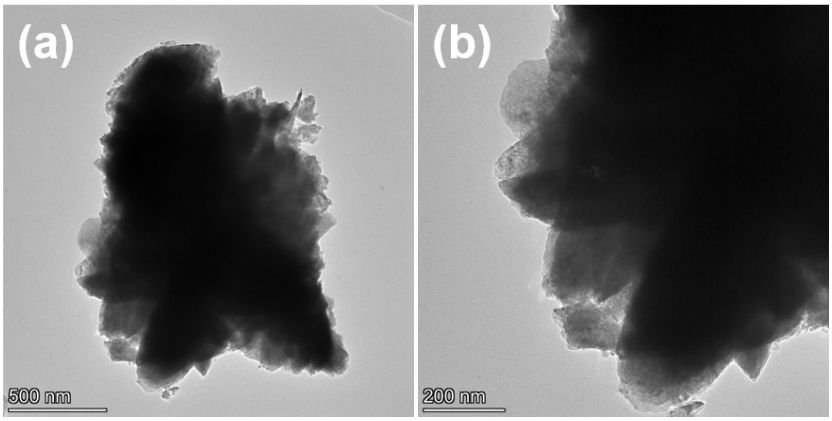

Fig. S6. The representative low- (a) and high- (b) magnification TEM images for CuO-2.

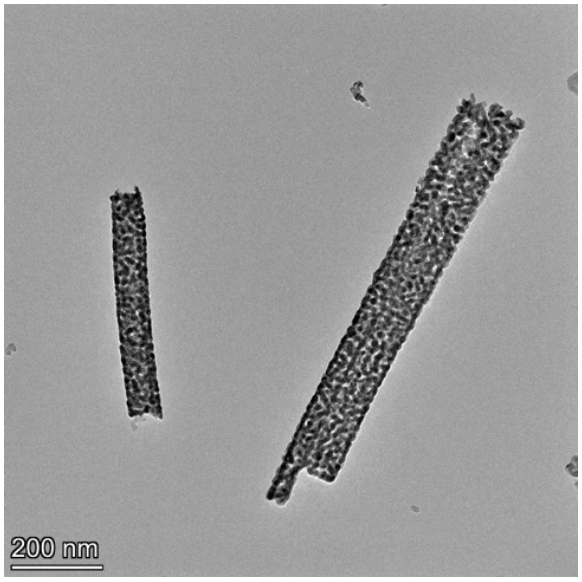

Fig. S7. TEM images of CuO-3.

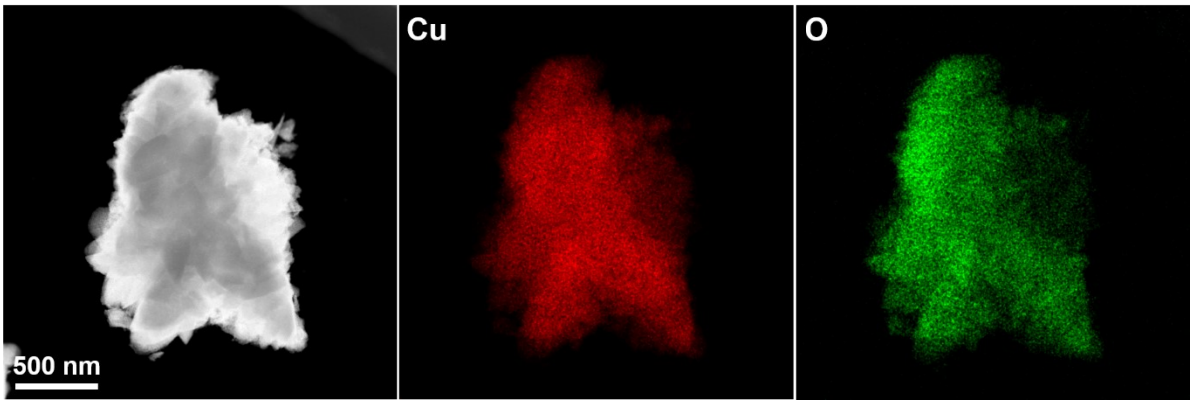

Fig. S8. HAADF-STEM image and the related elemental mapping patterns for CuO-2.

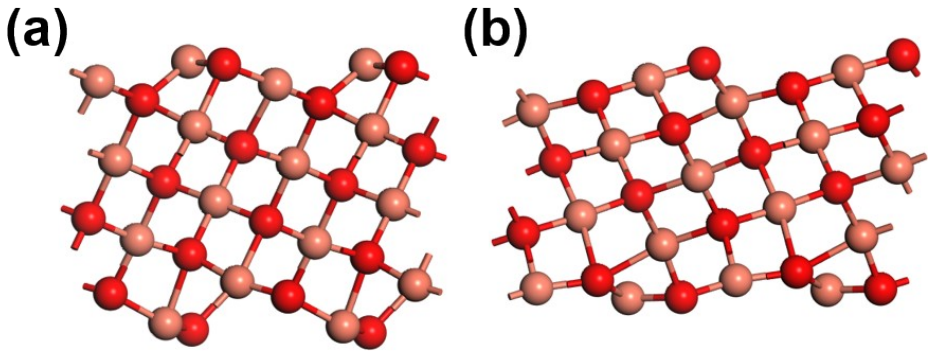

Fig. S9. The computational models for the (11-1) (a) and (111) (b) facets of CuO.

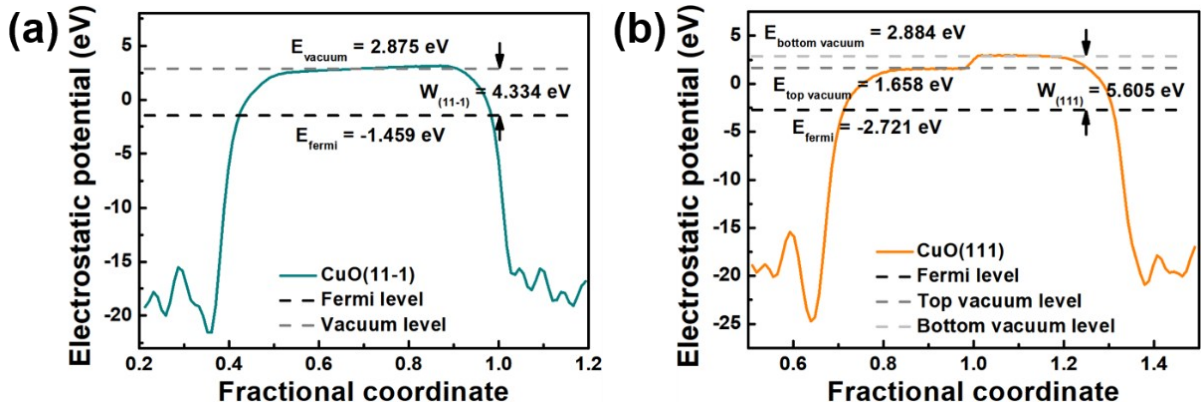

Fig. S10. The calculated work functions for the (11-1) (a) and (111) (b) facets of CuO.

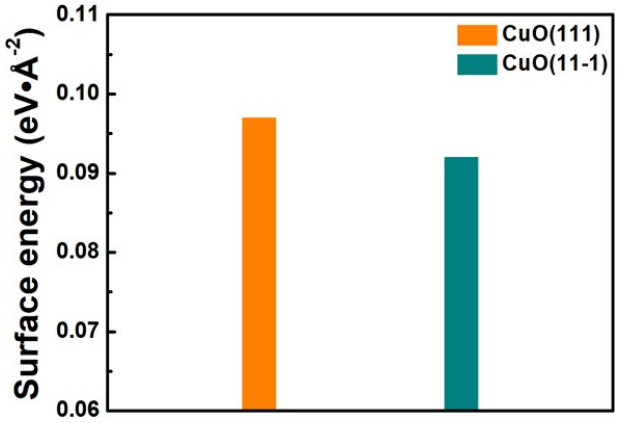

Fig. S11. The calculated surface energies for the (11-1) and (111) facets of CuO.

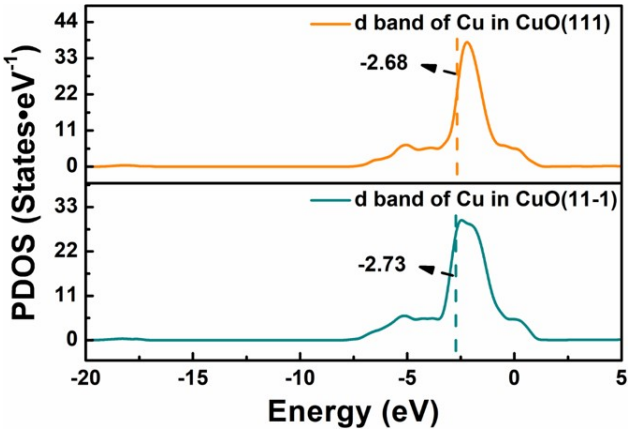

Fig. S12. The projected density of states of Cu 3d band for the (11-1) and (111) facets of CuO.

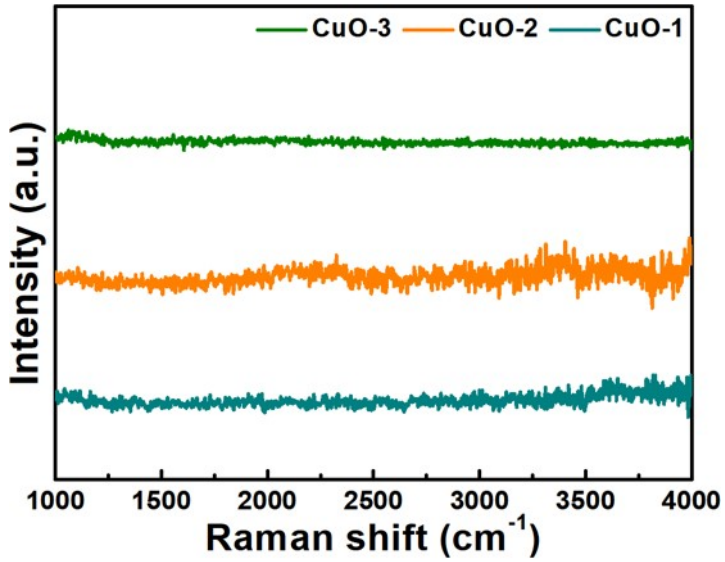

Fig. S13. Raman spectra for CuO-1, CuO-2, and CuO-3 at the wavenumber ranging from 1000 to 4000 cm^{-1}.

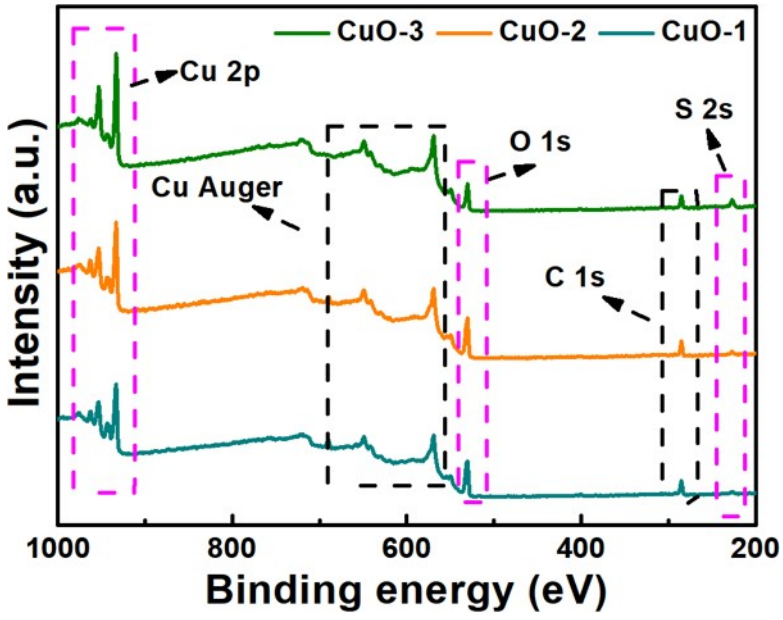

Fig. S14. The survey XPS spectra for CuO-1, CuO-2 and CuO-3.

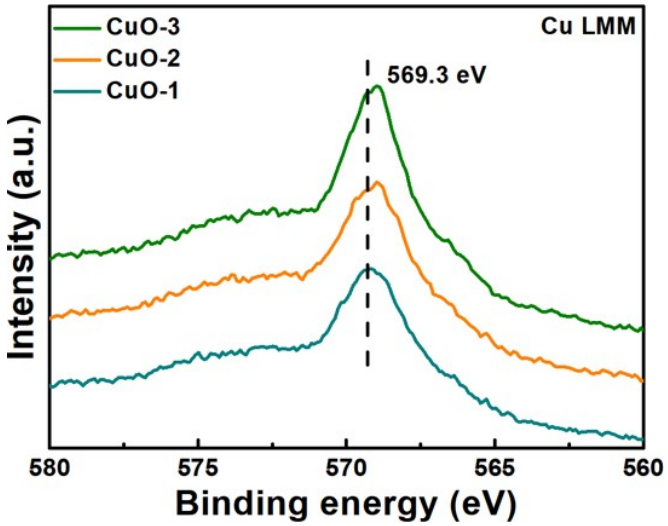

Fig. S15. The Cu LMM Auger spectra for CuO-1, CuO-2 and CuO-3.

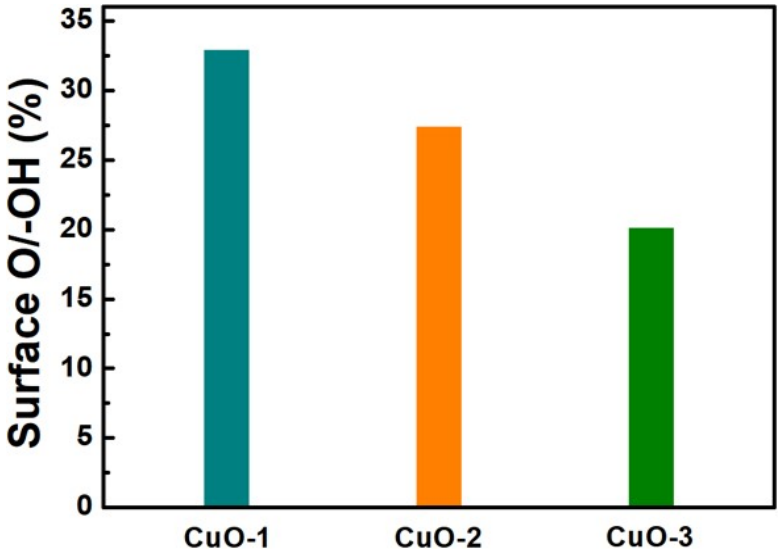

Fig. S16. The ratios of surface oxygen/-OH in CuO-1, CuO-2 and CuO-3.

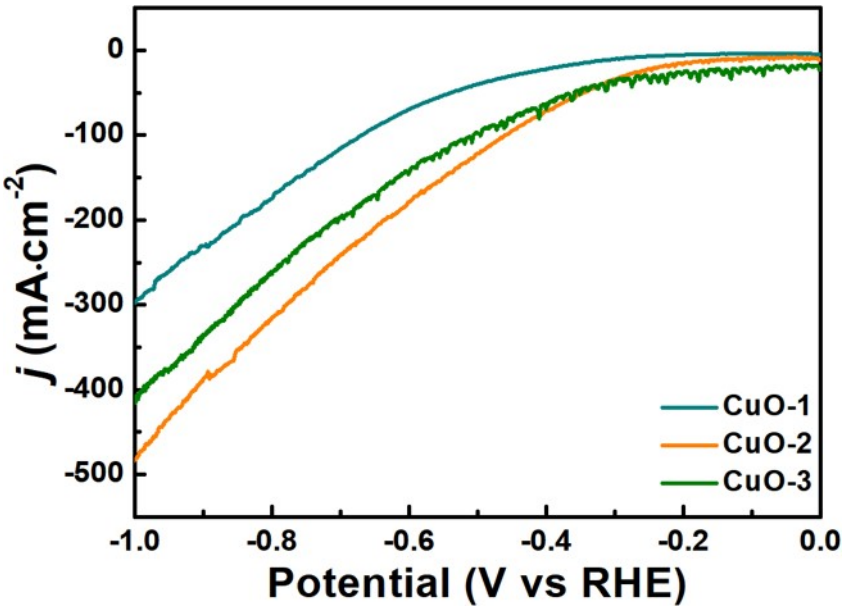

Fig. S17. LSV curves of CuO-1, CuO-2 and CuO-3.

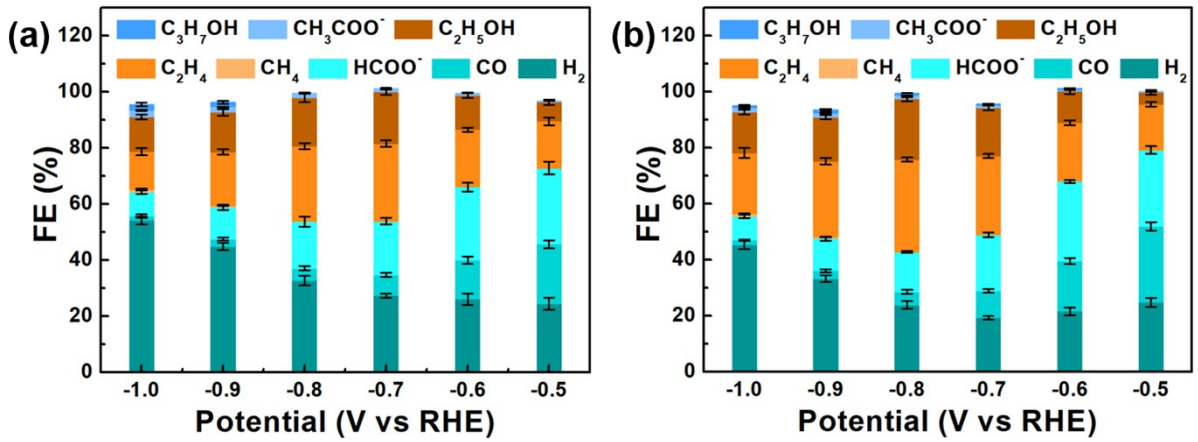

Fig. S18. FEs for products over CuO-3 (a) and CuO-1 (b) at various applied potentials in a flow cell reactor with 1.0 M KOH as the electrolyte.

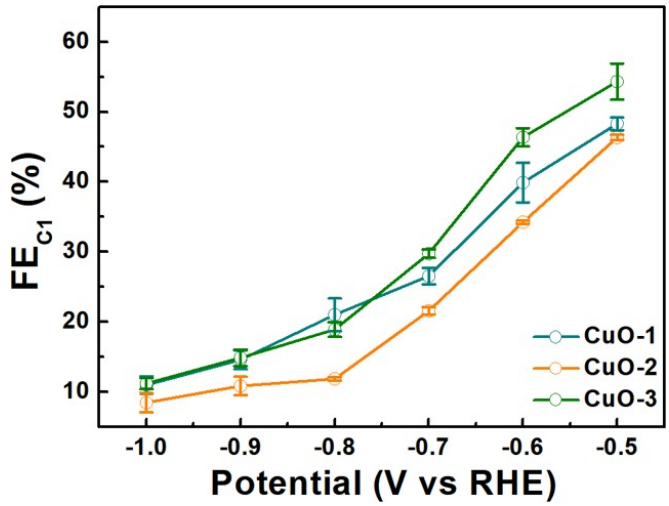

Fig. S19. FE_{C1} of CuO-1, CuO-2 and CuO-3 under various applied potentials.

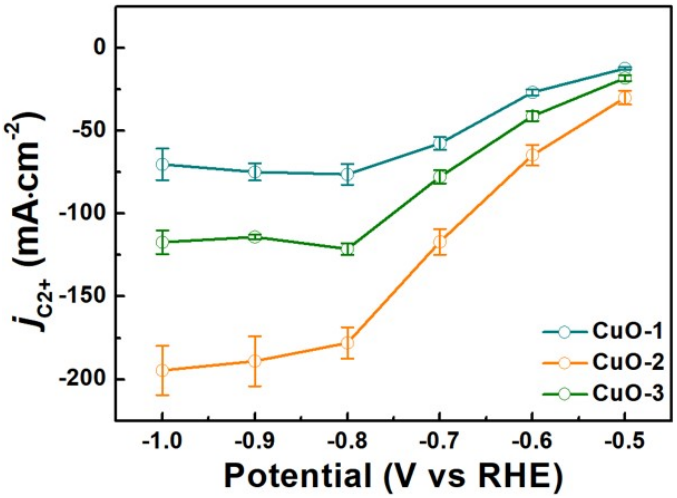

Fig. S20. Partial current density of C_{2+} products over CuO-1, CuO-2 and CuO-3 at various applied potentials.

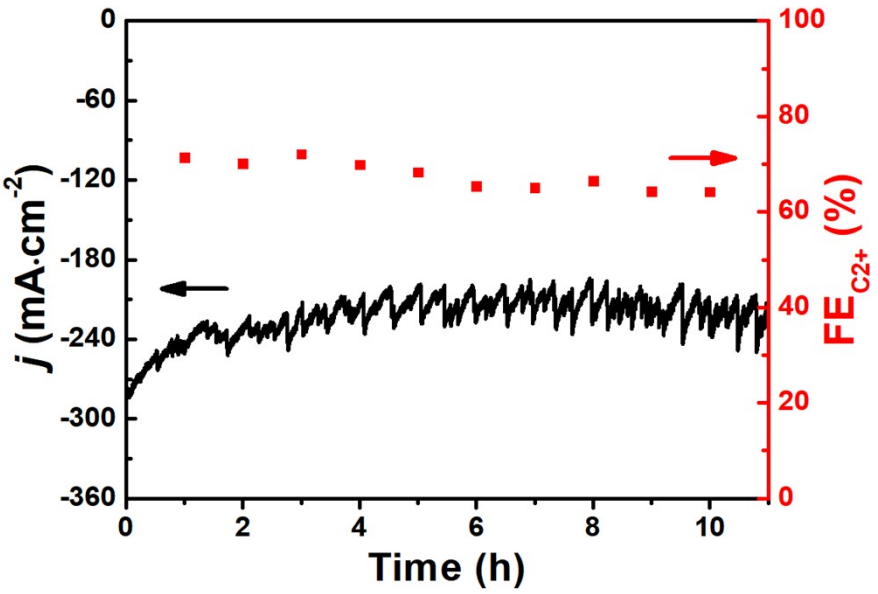

Fig. S21. Stability test of the CuO-2 at -0.8 V *vs*. RHE.

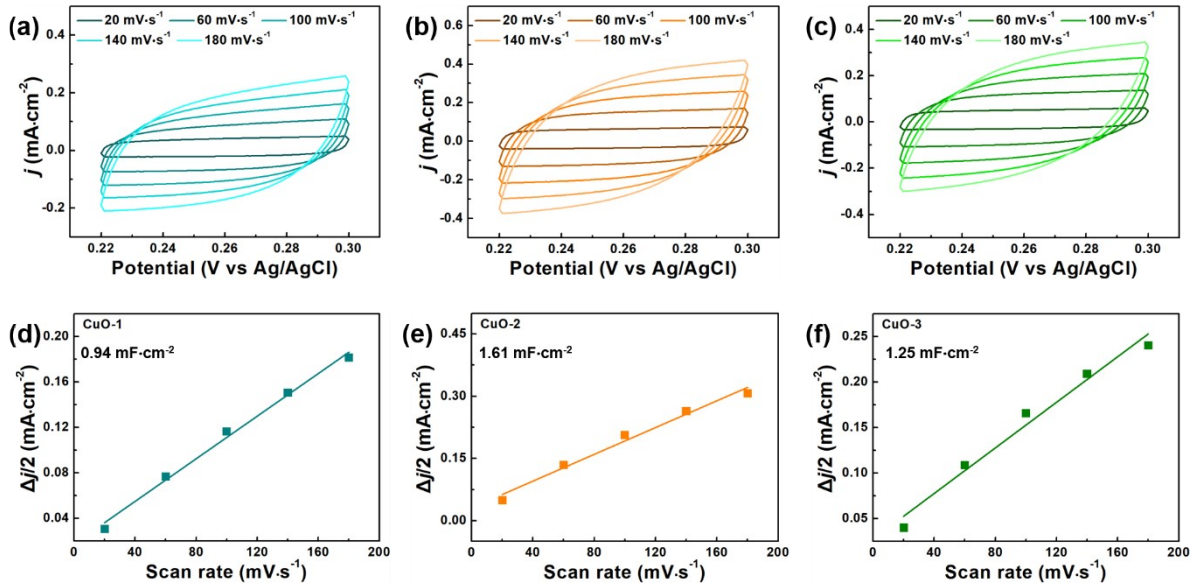

Fig. S22. (a-c) CV curves of CuO-1 (a), CuO-2 (b), and CuO-3 (c) from 0.22 to 0.3 V vs Ag/AgCl. (d-f) The corresponding C_{dl} plots for CuO-1 (d), CuO-2(e), and CuO-3 (f).

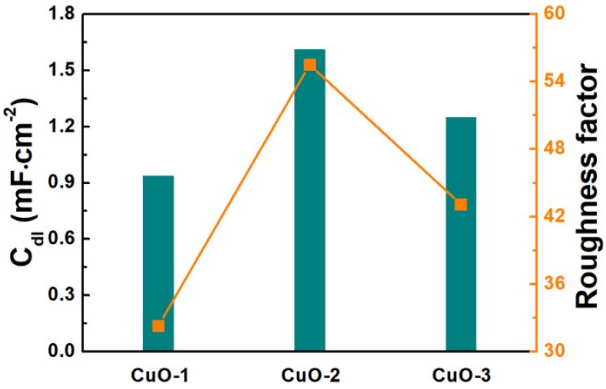

Fig. S23. The calculated roughness factors of CuO-1, CuO-2 and CuO-3.

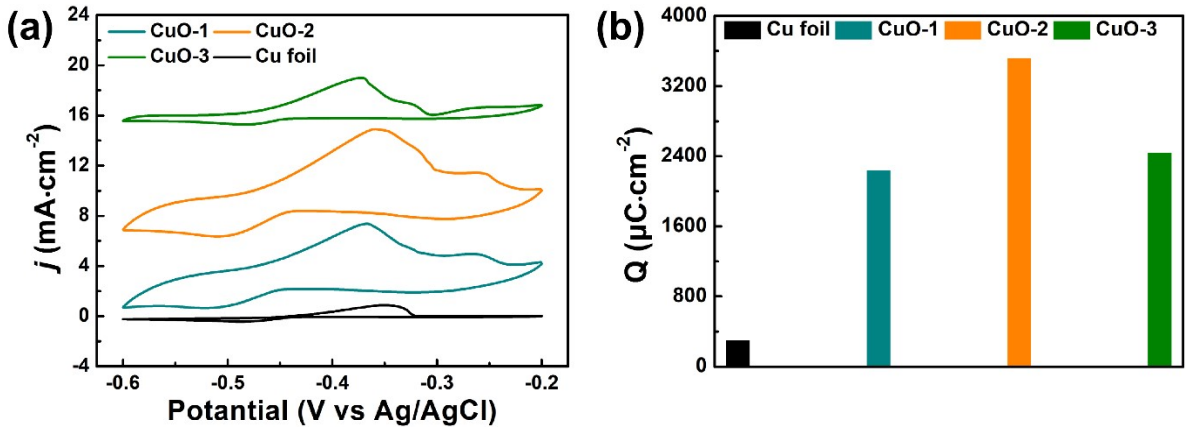

Fig. S24. CV curves (a) and the calculated Pb stripping charges (b) for CuO-1, CuO-2, CuO-3 and the reference Cu foil.

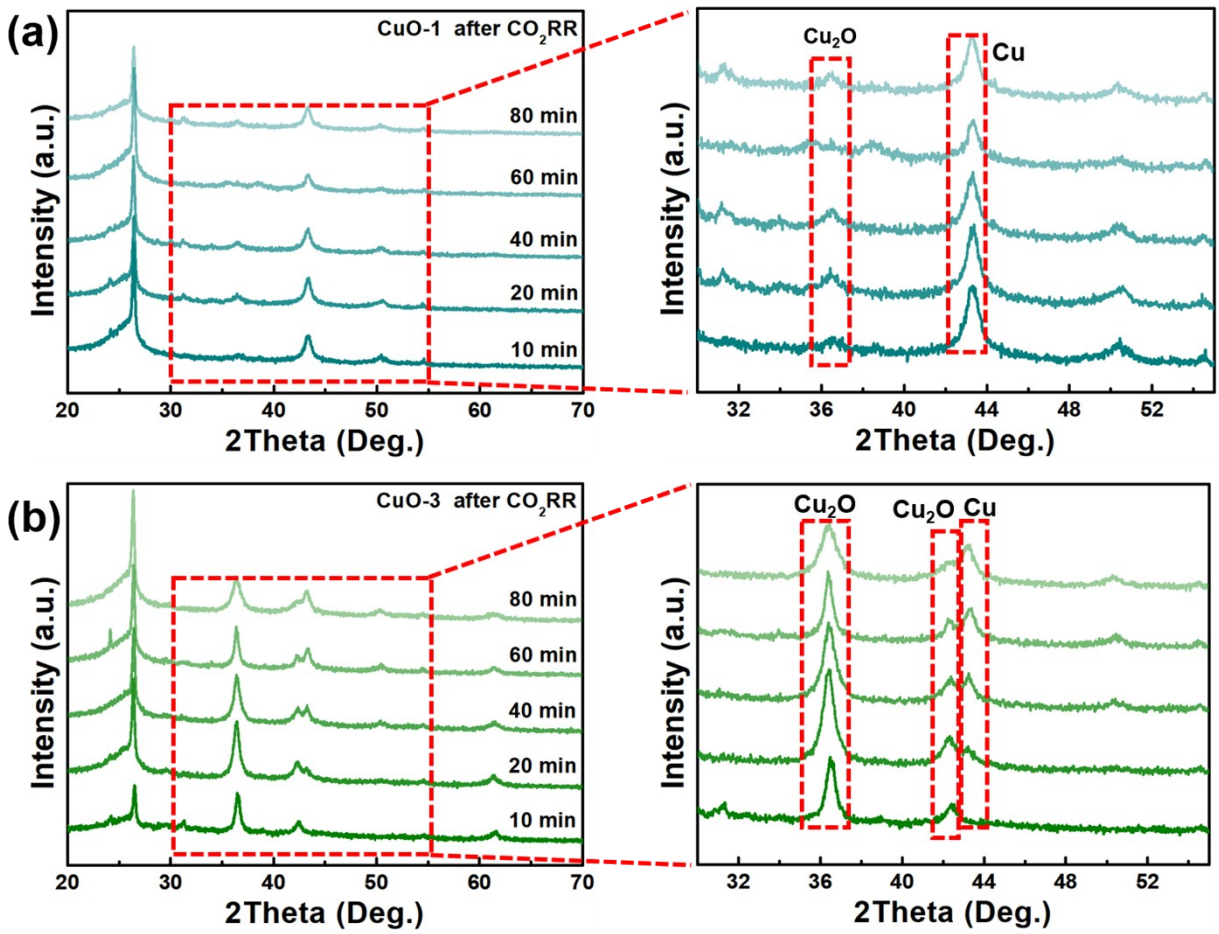

Fig. S25. XRD patterns of the collected CuO-1 (a) and CuO-3 (b) samples after CO_2RR at different reaction times.

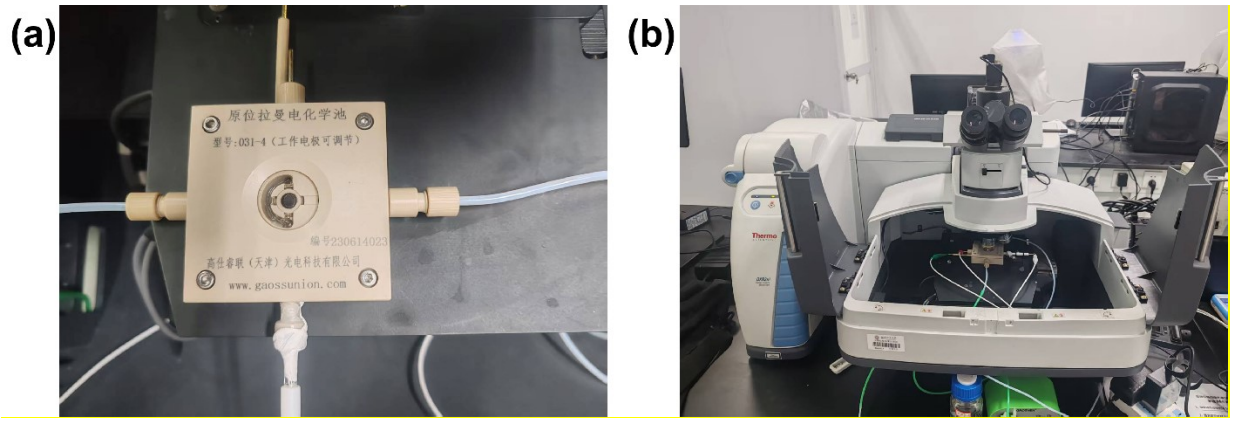

Fig. S26. The digital photographs for the configuration of the *in-situ* Raman cell (a) and the employed Raman experiment system (b).

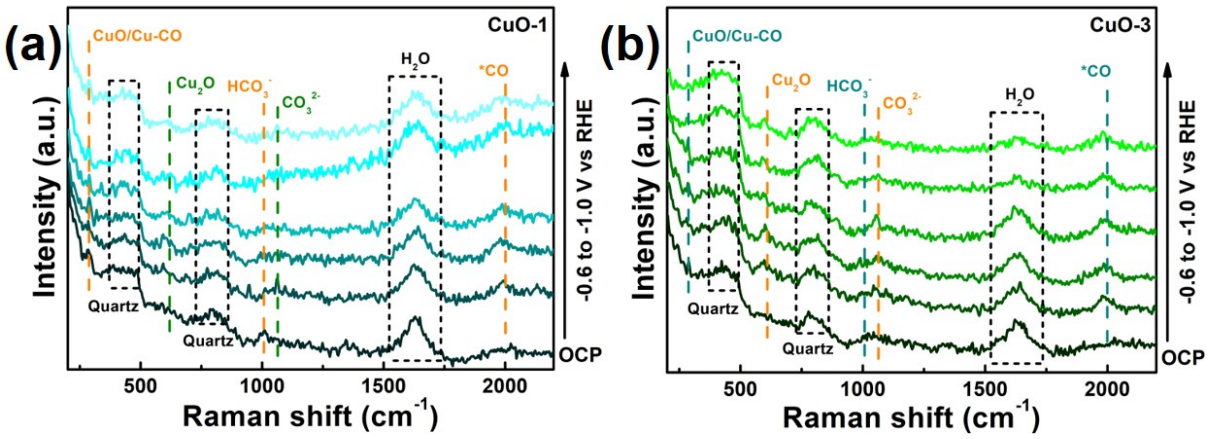

Fig. S27. The *In-situ* Raman spectra for CuO-1 (a) and CuO-3 (b) under varying applied potential.

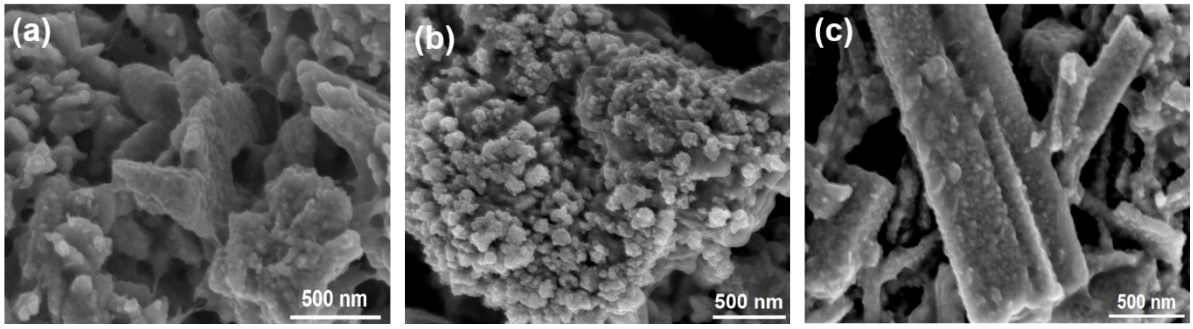

Fig. S28. The SEM images of CuO-1(a), CuO-2 (b) and CuO-3 (c) after CO_2RR.

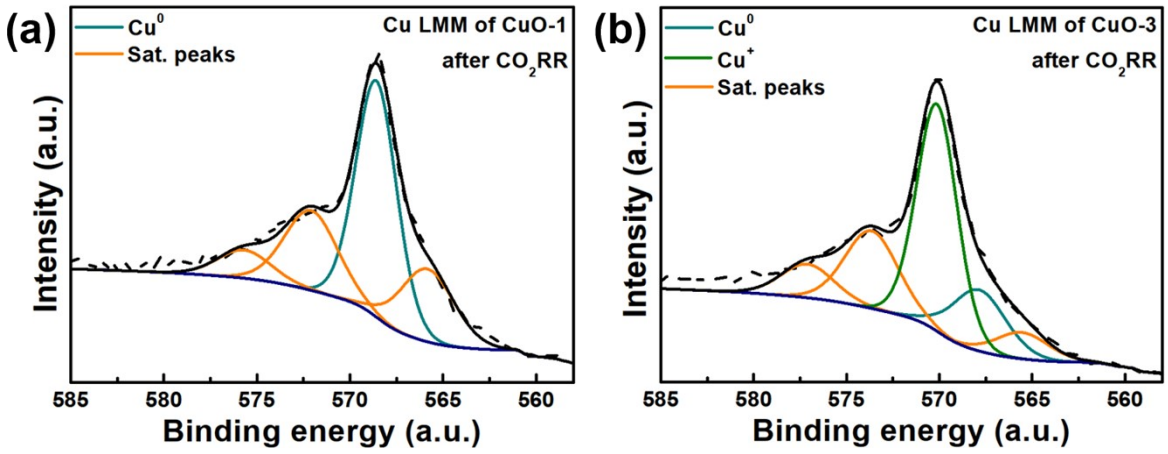

Fig. S29. Cu LMM Auger spectra of CuO-1(a) and CuO-3 (b) after CO_2RR.

References

1. Q. Li, J. Wu, L. Lv, L. Zheng, Q. Zheng, S. Li, C. Yang, C. Long, S. Chen and Z. Tang, *Adv. Mater.*, 2023, **36**, 2305508.
2. W. Chen, X. Jin, M. Wang, B. A, Z. Wei, G. Jiang, H. Shi and L. Zhang, *Adv. Funct. Mater.*, 2025, DOI: 10.1002/adfm.202526003.
3. J. Shao, P. Wei, S. Wang, Y. Song, Y. Fu, R. Li, X. Zhang, G. Wang and X. Bao, *Sci. China Mater.*, 2024, **67**, 1876-1881.
4. J. Jang, K. Lee, H. Shin, H. S. Lee, B.-H. Lee, J. Jeong, J. Kim, W. Hwang, S. Park, M. S. Bootharaju, S. Back, J. Shim, J. H. Kim, T. Hyeon and Y.-E. Sung, *J. Mater. Chem. A*, 2023, **11**, 19066-19073.